GPAV 1014815—13/2/2015—PRABHAKARAN.MN—506182——Style 4

International Journal of Pavement Engineering, 2015
Vol. 00, No. 0, 1–11, http://dx.doi.org/10.1080/10298436.2015.1014815

Assessing the effectiveness of probe vehicle acceleration measurements in estimating road roughness

Samer W. Katicha[a1], John El Khoury[b2]* and Gerardo W. Flintsch[a,c]

[a]*Virginia Tech Transportation Institute, Center for Sustainable Transportation Infrastructure, 3500 Transportation Research Plaza, Blacksburg, VA 24061, USA;* [b]*Department of Civil and Environmental Engineering, Lebanese American University, 211 East 46th Street, New York, NY 10017, USA;* [c]*Department of Civil and Environmental Engineering, Virginia Polytechnic Institute and State University, Blacksburg, VA 24061, USA*

[AQ1]

(*Received 23 September 2014; accepted 29 January 2015*)

In this article, we compare roadway roughness measured using a probe vehicle with roadway roughness calculated from the measured profile using an inertial profiler. Roughness is characterised by vehicle body vertical acceleration and probe vehicle roughness index (PVRI), which approximates the international roughness index (IRI) of a full car (rather than a quarter car). The reason the PVRI is used rather than the IRI is that acceleration measurements obtained from a probe vehicle represent the response of the full car rather than a quarter car. An important aspect of this article is that the same physical quantities are compared rather than obtaining a correlation between two different physical quantities. The results suggest that the roughness calculated from probe vehicle measurements is comparable with the roughness calculated from the measured profile; however, the investigation also revealed that data sampling frequency and quarter car parameters, specifically suspension damping and tyre stiffness, can have a significant effect on the measured PVRI.

Keywords: pavement monitoring; pavement roughness; probe vehicle; roadway profile; vehicle acceleration

1. Introduction

Recently, there has been a significant interest in obtaining pavement condition data from probe vehicles to use for asset management processes (El Khoury *et al.* 2014). Probe vehicles as defined in this study are vehicles that are instrumented to support naturalistic driving studies. Naturalistic data collection is the collection of driver behaviour and performance data in a natural environment. This *in situ* process uses drivers who operate vehicles that have been equipped with specialised sensors. Data regarding vehicle position, orientation, speed, acceleration, range, range rate, headway, time to collision, brake pedal input and qualitative data such as pre-incident manoeuvres can be used to describe the driver behaviour. One of the main reasons for this interest is that the probe vehicles form a sensory system greater in scale than any other data collection unit in the world (Ndoye *et al.* 2009). The data collected by probe vehicles would be dynamic and cover a large scope of the networks in which it is deployed to provide a constantly updating condition database (Eriksson *et al.* 2008).

An easily deployable probe vehicle application for pavement condition assessment is relating on-board vehicle acceleration sensors to ride quality. Ride quality, or smoothness, is one of the most vital condition indicators used by highway agencies and the driving pavement condition indicator in the public eye (Flintsch and McGhee 2009). Though other indicators have been investigated (Loizos and Plati 2008), the most commonly used measure to report ride quality in the USA is the international roughness index (IRI). The IRI was developed by the National Cooperative Highway Research Program and the World Bank (Sayers and Karamihas 1998). Because of the wide use of IRI as pavement roughness indicator, it has become the standard to evaluate the effectiveness of probe vehicle measurements in obtaining roughness indicators. A recent example is the report by Dawkins *et al.* (2011) which is part of the Intellidrive[SM] study. The report correlated probe vehicle root mean square acceleration measurements, as well as another indicator called 'pseudo IRI' (PIRI), with IRI measurements obtained using an inertial profiler. The PIRI – defined as the probe vehicle suspension travel – was directly measured. One disadvantage of the PIRI is that it is unlikely that deployed vehicles on the roadways would have sensors that measure the suspension travel. Rather, it is much more likely and readily available to measure vehicle body acceleration of deployed probe vehicles. In this article, we evaluate the ability to estimate the pavement roughness using probe vehicle body acceleration measurements. This is done by comparing the probe vehicle roughness index (PVRI) and vertical accelerations with PVRI and vertical accelerations obtained using inertial profiler. The objective is to compare probe vehicle measurements and profiler measurements

*Corresponding author. Email: john.khoury@lau.edu.lb

GPAV 1014815—13/2/2015—PRABHAKARAN.MN—506182——Style 4

using the same physical quantities, namely the PVRI and vehicle vertical acceleration. The PVRI is an approximation of the IRI, having the same units of measurements. The reason the PVRI is used in this study rather than the IRI is that acceleration measurements obtained from a probe vehicle represent the response of a full car rather than a quarter car – which is the standard method used to obtain the IRI. By using the same physical quantities, the agreement and differences between the two measurement methods can be more clearly identified. Probe vehicle acceleration measurements were used to back-calculate the PVRI which can also be obtained from the measured profile.

2. Objective

Roughness measures obtained from the probe vehicle are compared with roughness measures obtained from the roadway measured profile. Using the probe vehicle on-board acceleration measurements, the pavement PVRI is back-calculated and compared with the PVRI obtained from the roadway profile. We also calculate the hypothetical vehicle acceleration from profile measurements and compare it to the probe vehicle measured acceleration. Many studies have correlated on-board acceleration measurements with pavement IRI. In this article, we compare two quantities with the same physical units, obtained using the quarter car model. The quarter car model has already been effectively used to obtain roadway roughness measures from the measured profile. We present a numerical approach to obtain roadway roughness measures from measured vehicle vertical acceleration.

The probe vehicle used in this study is a 2007 Ford Fusion. This vehicle has quarter car parameters similar to the golden car parameters used to calculate the IRI. For this purpose, we have assumed that the golden car parameters are reasonable parameters to be used with the probe vehicle. We also performed a sensitivity analysis by changing the golden car parameters by up to 25% to determine the effect this will have on the calculated PVRI.

3. Differences between probe vehicle and quarter car model

An important difference between the probe vehicle measurements and the quarter car model is that the probe vehicle vertical acceleration is obtained as the response of the full car and not just the quarter car; hence, the term PVRI rather than IRI. The probe vehicle measurements capture the left and the right wheel paths vertical acceleration profiles and also sense the roadway roughness through the front and back tyres, all at the same time. Therefore, the response of the probe vehicle is the average of the response of all four tyres. This response is best obtained through a full car model. However, for the purpose of our application, the full car model is too complicated for the level of accuracy required. We choose to approximate the full car response to the roadway profile as follows:

(1) Average the left and right wheel paths roadway profiles.
(2) Average the response of the roadway profile with a copy of it, shifted by a distance equal to the vehicle wheelbase. This average is used to represent the average response of the vehicle based on the front and back tyres.
(3) Calculate the PVRI using the quarter car model with the averaged roadway profile according to 1 and 2.

These approximations simplify the problem yet they are adequate for the intended application. For more accuracy, a precise measure of the accelerometer location inside the probe vehicle is needed along with an accurate estimate of the model car parameters. These parameters include the suspension stiffness and damping, tyre stiffness and damping, as well as inflation pressure for a wide range of cars travelling on the road. To obtain these parameters accurately, extensive efforts are needed. This defies the purpose of using the probe vehicle data, which are readily available to obtain and thus could be considered as a practical alternative to dedicated equipment for network level evaluation.

4. Methodology

Vertical acceleration and PVRI obtained from the probe vehicle are compared to vertical acceleration and PVRI measurement calculated from the inertial profiler:

(1) Vehicle vertical acceleration is selected for the following reasons: (1) it is a direct measurement from the probe vehicle, (2) it is easily obtained from the measured roadway profile, and (3) it is a reasonable measure of what the travelling public experience.
(2) PVRI is selected because it is similar to the IRI, which is a widely used measure of roughness in the USA.

Before going into the details of the comparison, we highlight two issues related to data sampling that can have a profound effect on the calculation of roughness. We do so because measurements collected by the probe vehicle were obtained every 2200 mm while measurements collected by the inertial profiler were obtained every 30 mm. The first issue is the numerical implementation of the quarter car model, which is essentially a differential equation. Its numerical solution accuracy depends on the discretisation interval. The required interval for adequate accuracy depends on the quarter car model parameters. For the golden car parameters, this interval should be

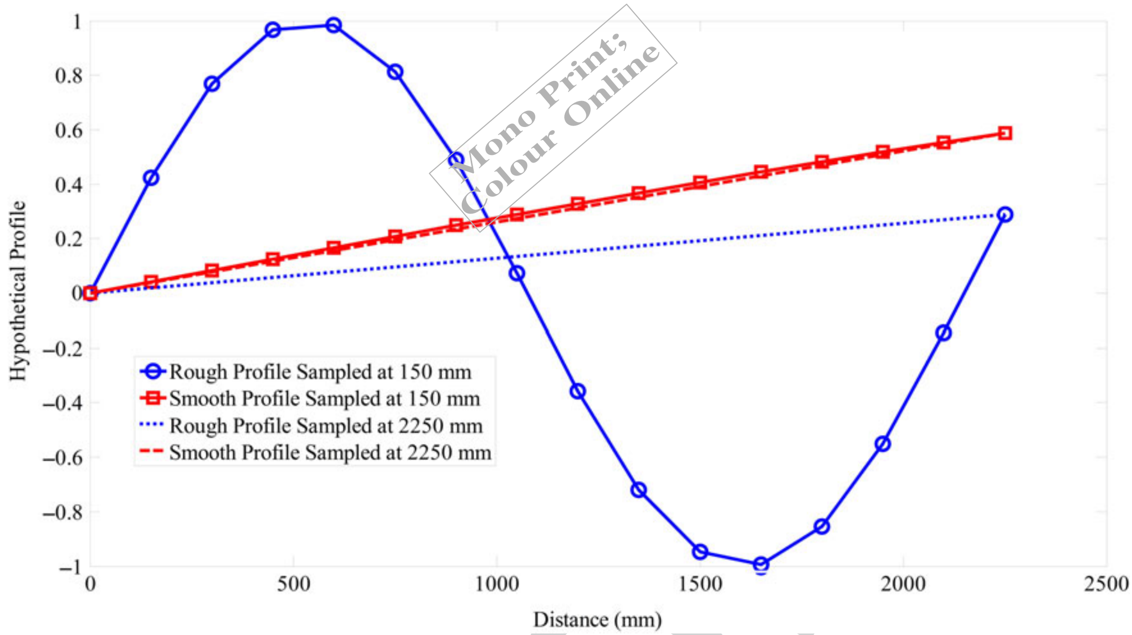

Figure 1. Effect of sampling interval on measured profile.

<250 mm (10 in.) and in general, inertial profilers collected measurements at 150 mm (6 in.) intervals or lower. Profile measurements used in this article were obtained at about 30 mm (1.2 inch) intervals, which provides for accurate calculations. Figure 1 shows two hypothetical profiles, one smooth and one rough, obtained at 150 mm intervals over a 2250 mm roadway section (we chose 2250 mm and not 2200 mm because 2250 mm is a multiple of 150 mm).

For the smooth profile, sampling performed at 2250 mm interval led to no significant loss of profile features compared to sampling at 150 mm. An interval of 2200 mm is, however, too large for numerical discretisation of the differential equation. Thus, measurements obtained at 2250 mm can be interpolated so that the numerical implementation of the quarter car model can be performed at 150 mm (or at least 250 mm). As for the rough profile, sampling at 2250 mm missed important profile features, as shown in Figure 1. Even though interpolation is used to achieve better numerical accuracy, it will not recover the important features that are lost due to the large sampling interval (2250 mm). That will lead to a loss of accuracy in IRI calculation due to the loss of information.

The difference in the sampling interval between the probe vehicle and the inertial profiler should be accounted for to fairly compare the roughness measurements obtained from each vehicle. This is discussed in detail in Section 6 of this article. In future, we recommend that probe vehicle acceleration measurements be obtained at a sampling rate that is similar to the profile measurement sampling rate.

The remainder of the article addresses the following:

(1) Present the quarter car model numerical calculations. IRI calculation from roadway profile is well known (Sayers and Karamihas 1996) and we therefore concentrate on IRI calculation from vehicle body acceleration measurements.
(2) Evaluate the accuracy of the numerical calculation of IRI from vehicle acceleration measurements.
(3) Evaluate the effects of data sampling intervals (2200 mm vs. 30 mm) on the calculated IRI based on the roadway profile which was back-calculated from vehicle acceleration.
(4) Evaluate the effect of averaging the roadway profile (left and right as well as front and back) on vehicle acceleration calculated from the roadway profile.
(5) Compare vertical acceleration calculated from the roadway profile with probe vehicle measured acceleration.
(6) Compare the PVRI calculated from the probe vehicle to the PVRI calculated from profile measurements.
(7) Perform a sensitivity analysis of the calculated PVRI from the roadway profile with respect to acceleration sampling location.
(8) Perform a sensitivity analysis of the calculated PVRI from the probe vehicle acceleration measurements with respect to the quarter car model parameters.

5. Background

5.1. *The quarter car model*

Calculation of the IRI is based on the quarter car model shown in Figure 2. [AQ2] In this model, $\mathbf{z}_{\text{road}}$ represents the profile, $\mathbf{z}_{\text{tyre}}$ the vertical movement of the tyre, $\mathbf{z}_{\text{body}}$ the vertical movement of the vehicle body, k_{b} the suspension stiffness coefficient, C_{b} the suspension damping coefficient and k_{t} the tyre stiffness. The basic equations of the quarter car model that relate the vehicle body and tyre vertical movements to the road profile are presented in Equations (1) and (2). These two equations are most conveniently written in a matrix form as shown in Equation (3) (see Sayers and Karamihas 1996).

$$M_{\text{body}}\ddot{z}_{\text{body}} = C_{\text{b}}(\dot{z}_{\text{tyre}} - \dot{z}_{\text{body}}) + k_{\text{b}}(z_{\text{tyre}} - z_{\text{body}}), \quad (1)$$

$$M_{\text{tyre}}\ddot{z}_{\text{tyre}} = -C_{\text{b}}(\dot{z}_{\text{tyre}} - \dot{z}_{\text{body}}) - k_{\text{b}}(z_{\text{tyre}} - z_{\text{body}}) + k_{\text{t}}(z_{\text{road}} - z_{\text{tyre}}), \quad (2)$$

$$\begin{bmatrix} \dot{\mathbf{z}}_{\text{body}} \\ \ddot{\mathbf{z}}_{\text{body}} \\ \dot{\mathbf{z}}_{\text{tyre}} \\ \ddot{\mathbf{z}}_{\text{tyre}} \end{bmatrix} = \begin{bmatrix} 0 & 1 & 0 & 0 \\ -k_1 & -C & k_1 & C \\ 0 & 0 & 0 & 1 \\ \frac{k_1}{\mu} & \frac{C}{\mu} & -\frac{k_1+k_2}{\mu} & -\frac{C}{\mu} \end{bmatrix} \begin{bmatrix} \mathbf{z}_{\text{body}} \\ \dot{\mathbf{z}}_{\text{body}} \\ \mathbf{z}_{\text{tyre}} \\ \dot{\mathbf{z}}_{\text{tyre}} \end{bmatrix} + \begin{bmatrix} 0 \\ 0 \\ 0 \\ \frac{k_2}{\mu} \end{bmatrix} \mathbf{z}_{\text{road}}, \quad (3)$$

where

$$k_1 = \frac{k_{\text{b}}}{M_{\text{body}}},$$

$$k_2 = \frac{k_{\text{t}}}{M_{\text{tyre}}},$$

$$C = \frac{C_{\text{b}}}{M_{\text{body}}} \quad \text{and}$$

$$\mu = \frac{M_{\text{tyre}}}{M_{\text{body}}}.$$

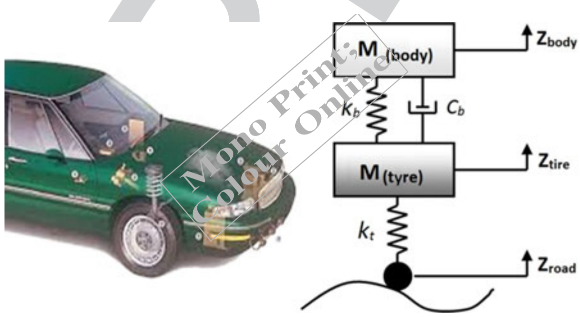

Figure 2. Quarter car model.

Details on how to solve Equation (3) can be found in Loizos and Plati (2008).

The IRI is defined as follows:

$$\text{IRI} = \frac{1}{n}\sum_{i=1}^{n} |\mathbf{s}_{\text{body},i} - \mathbf{s}_{\text{tyre},i}|, \quad (4)$$

where

$$\mathbf{s} = \frac{\mathrm{d}\mathbf{z}}{\mathrm{d}x},$$

with n chosen to include 528 ft.

For a probe vehicle, $\ddot{\mathbf{z}}_{\text{body}}$ is directly measured from which the roadway roughness or an index similar to the IRI is calculated. For this reason, we need to determine a profile that will result in essentially the same IRI as the one calculated from the roadway profile obtained from the inertial profiler. Note that we do not need to recover the exact road profile but a profile that will result in the same vehicle body acceleration and IRI. Even with inertial profilers, when different makes are used on the same roadway section, slightly different profiles are obtained mainly due to calibration and human elements; yet the variations between measurements are insignificant for the purpose of the application.

Starting with the measurements of the vehicle body vertical acceleration $\ddot{\mathbf{z}}_{\text{body}}$, the vehicle body vertical speed $\dot{\mathbf{z}}_{\text{body}}$ is obtained. Assuming $\ddot{\mathbf{z}}_{\text{body}}$ changes linearly between two measurements, over the sampling interval Δt, $\dot{\mathbf{z}}_{\text{body}}$ can be calculated as follows:

$$\begin{aligned} \dot{\mathbf{z}}_{\text{body}}(\mathbf{i}+\mathbf{1}) &= \dot{\mathbf{z}}_{\text{body}}(\mathbf{i}) + \int_0^{\Delta t}\left[\ddot{\mathbf{z}}_{\text{body}}(\mathbf{i}) + \frac{\ddot{\mathbf{z}}_{\text{body}}(\mathbf{i}+\mathbf{1}) - \ddot{\mathbf{z}}_{\text{body}}(\mathbf{i})}{\Delta t}t\right]\mathrm{d}t \\ &= \dot{\mathbf{z}}_{\text{body}}(\mathbf{i}) + \ddot{\mathbf{z}}_{\text{body}}(\mathbf{i})\Delta t + \frac{\ddot{\mathbf{z}}_{\text{body}}(\mathbf{i}+\mathbf{1}) - \ddot{\mathbf{z}}_{\text{body}}(\mathbf{i})}{2}\Delta t \\ &= \dot{\mathbf{z}}_{\text{body}}(\mathbf{i}) + \frac{\ddot{\mathbf{z}}_{\text{body}}(\mathbf{i}+\mathbf{1}) + \ddot{\mathbf{z}}_{\text{body}}(\mathbf{i})}{2}\Delta t, \end{aligned} \quad (5)$$

with $\mathbf{i} = 1, \ldots, n$ and n is the number of measurements. Similarly, $\mathbf{z}_{\text{body}}$ can be obtained by integration as follows:

$$\mathbf{z}_{\text{body}}(\mathbf{i}+\mathbf{1}) = \mathbf{z}_{\text{body}}(\mathbf{i}) + \dot{\mathbf{z}}_{\text{body}}(\mathbf{i})\Delta t + \frac{\ddot{\mathbf{z}}_{\text{body}}(\mathbf{i}+\mathbf{1}) + 2\ddot{\mathbf{z}}_{\text{body}}(\mathbf{i})}{6}\Delta t^2. \quad (6)$$

Using Equation (1), $\dot{\mathbf{z}}_{\text{tyre}}$ is obtained as follows:

$$\dot{\mathbf{z}}_{\text{tyre}}(\mathbf{i}+\mathbf{1}) = \frac{\ddot{\mathbf{z}}_{\text{body}}(\mathbf{i}+\mathbf{1}) + \ddot{\mathbf{z}}_{\text{body}}(\mathbf{i})}{2C} + \frac{k_1}{C}(\mathbf{z}_{\text{body}}(\mathbf{i}) - \mathbf{z}_{\text{tyre}}(\mathbf{i})) + \dot{\mathbf{z}}_{\text{body}}(\mathbf{i}). \quad (7)$$

And assuming $\dot{\mathbf{z}}_{\text{tyre}}$ changes linearly over the sampling interval Δt, $\mathbf{z}_{\text{tyre}}$ is calculated as follows:

$$\mathbf{z}_{\text{tyre}}(\mathbf{i}+\mathbf{1}) = \mathbf{z}_{\text{tyre}}(\mathbf{i}) + \frac{\dot{\mathbf{z}}_{\text{tyre}}(\mathbf{i}+\mathbf{1}) + \dot{\mathbf{z}}_{\text{tyre}}(\mathbf{i})}{2}\Delta t. \quad (8)$$

The profile $\mathbf{z}_{\text{road}}$ can then be obtained as follows:

$$\begin{aligned}\mathbf{z}_{\text{road}}(\mathbf{i}+\mathbf{1}) = {} & \frac{\mu}{k_1}\frac{\dot{\mathbf{z}}_{\text{tyre}}(\mathbf{i}+\mathbf{1}) - \dot{\mathbf{z}}_{\text{tyre}}(\mathbf{i})}{\Delta t} \\ & - \frac{k_2}{\mu}\frac{\mathbf{z}_{\text{body}}(\mathbf{i}+\mathbf{1}) + \mathbf{z}_{\text{body}}(\mathbf{i})}{2} \\ & - \frac{C}{\mu}\frac{\dot{\mathbf{z}}_{\text{body}}(\mathbf{i}+\mathbf{1}) + \dot{\mathbf{z}}_{\text{body}}(\mathbf{i})}{2} \\ & + \frac{k_1+k_2}{\mu}\frac{\mathbf{z}_{\text{tyre}}(\mathbf{i}+\mathbf{1}) + \mathbf{z}_{\text{tyre}}(\mathbf{i})}{2} \\ & + \frac{C}{\mu}\frac{\dot{\mathbf{z}}_{\text{tyre}}(\mathbf{i}+\mathbf{1}) + \dot{\mathbf{z}}_{\text{tyre}}(\mathbf{i})}{2}. \end{aligned} \quad (9)$$

The calculated road profile from Equation (9) can be used to calculate the IRI using Equations (3) and (4).

5.2. *Accuracy of the equations*

When comparing roughness measures from the probe vehicle acceleration measurements with those obtained from the measured profile, it is crucial to verify that observed discrepancies are not due to the numerical accuracy of the equations used in the calculation. A simple and effective way to evaluate the accuracy of the equations is to first calculate the IRI using the measured roadway profile and Equations (3) and (4). This is how the IRI is actually calculated. From this procedure, the quarter car vehicle body acceleration $\ddot{\mathbf{z}}_{\text{body}}$ is obtained as well. The calculated $\ddot{\mathbf{z}}_{\text{body}}$ can in turn be used to recalculate a road profile $\mathbf{z}_{\text{road}}$ using Equations (5)–(9). The road profile $\mathbf{z}_{\text{road}}$ is then used to back-calculate IRI using Equations (3) and (4). The back-calculated IRI is compared with the IRI obtained from the measured profile. An example of such comparison is shown in Figure 3, which presents IRI computation performed on the Virginia Smart Road. The original IRI and the back-calculated IRI graphs cannot practically be distinguished. The difference between the two calculated IRI values is also shown in Figure 3. The difference is insignificant as it is much smaller than what would be obtained from repeated runs of road profile measurements. This shows that the numerical procedure is accurate enough and can be used to compare the PVRI calculated from the probe vehicle acceleration measurements and PVRI calculated from road profile measurements. Any differences that might be observed would not be due to numerical errors in the discretisation of the quarter car model.

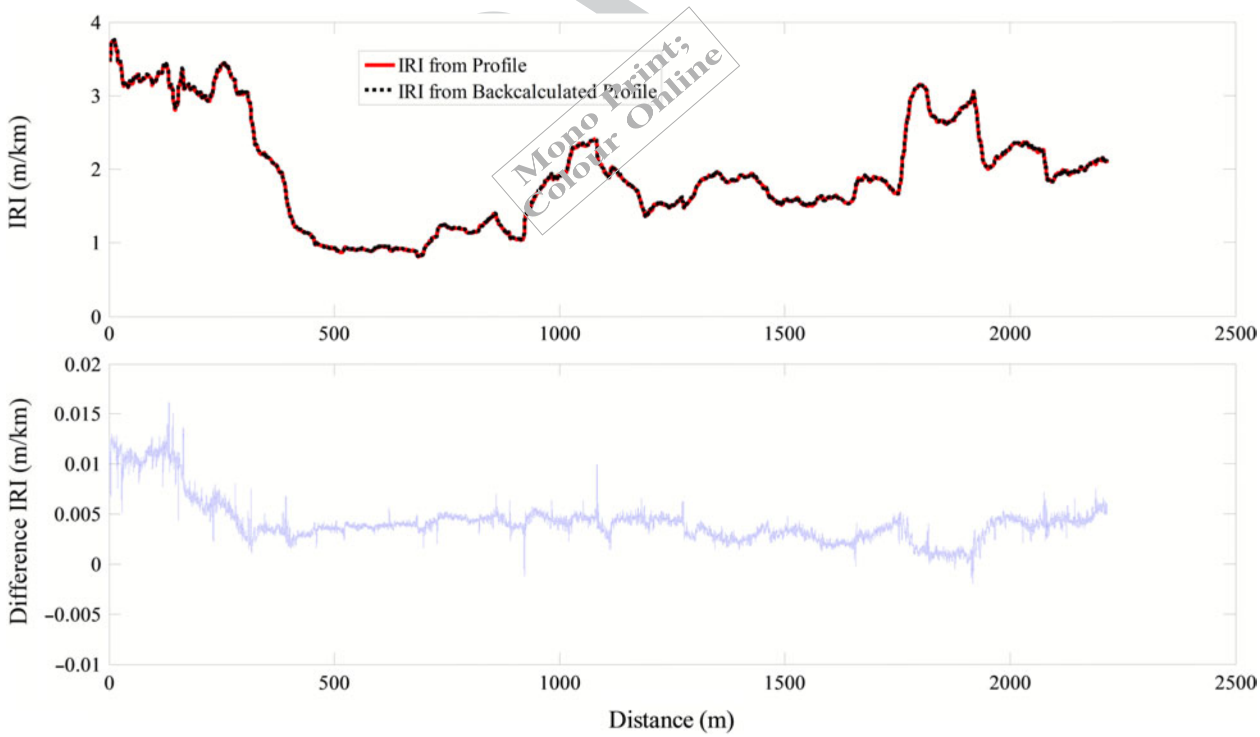

Figure 3. Accuracy of IRI calculation: calculated IRI (top) and difference between calculated IRI (bottom).

6. Results and analysis

6.1. *Response of average left and right wheel path profiles*

To evaluate the pavement roughness, we first perform the calculation with the averaged left and right wheel path profiles but without averaging the response of the front and back axles (tyres). This approach is the one usually followed to calculate the half-car roughness index. Figure 4 shows the accelerations calculated from the profile (left and right wheel path average) using the quarter car model (with the golden car parameters) and the probe vehicle measured accelerations. Note that the calculated acceleration is based on a profile initially sampled at 30 mm (1.2 in.) and then re-sampled at 2200 mm to match the sampling interval of the probe vehicle. Both accelerations (probe vehicle measured and profile calculated) have similar features. To measure how much the acceleration sets agree, the Pearson correlation coefficient between the two data-sets was calculated to be 0.73. Note that Flintsch *et al.* (2012) calculated the correlation between the profile and acceleration measurements at 0.50. Clearly, converting the profile to acceleration increases the correlation as similar physical quantities are being compared.

Although the two vehicle vertical acceleration profiles look similar, there are still noticeable differences. In general, the probe vehicle measured acceleration is 'smoother' than the calculated acceleration from the measured road profile (note in Figure 4 the area between 0 and 400 m or the large peak at approximately 1750 m). To summarise the difference in acceleration values, we can calculate the signal average strength in terms of its average norm (root mean square) as follows:

$$S = \frac{\sqrt{\left(\sum_{i=1}^{n} m_i\right)}}{n},$$

where S is the average norm (signal strength), m_i is the individual measurement and n is the total number of measurements. For the profile-calculated accelerations, the signal average strength is 0.56 m/s^2 while the average strength of the probe vehicle measured accelerations is 0.45 m/s^2, which represents a 20% drop.

Three PVRI sets are presented in Figure 5. The first PVRI is back-calculated from the probe vehicle measured accelerations. The other two PVRI sets are calculated from the measured road profile. For the latter two PVRI sets, the first is directly calculated from the measured road profile at 30 mm sampling interval using the inertial profiler. This PVRI coincides with the IRI. The second profile PVRI is obtained as follows: (1) calculate the quarter car body vertical acceleration, (2) sample this acceleration at 2200 mm and (3) back-calculate the PVRI from the sampled accelerations. In Step 2, sampling is performed at 2200 mm to match the sampling rate of the probe vehicle. The PVRI calculated by sampling the calculated vehicle

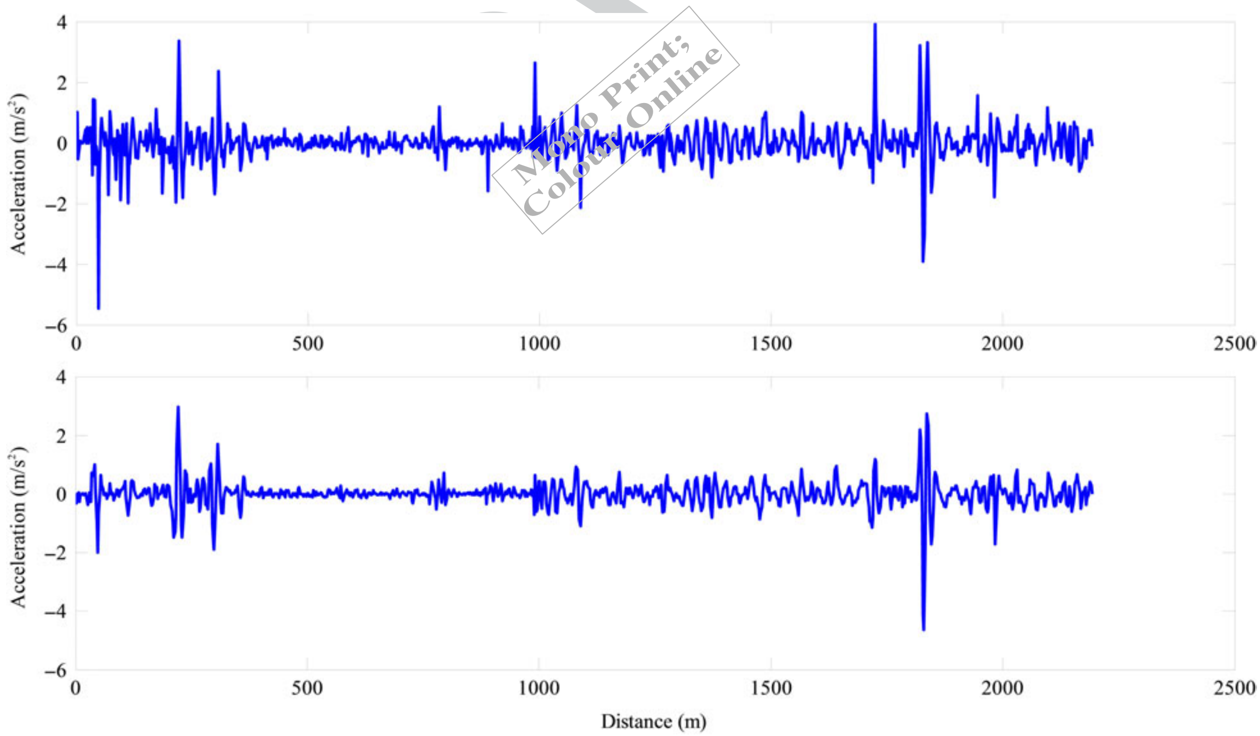

Figure 4. Vehicle vertical acceleration, top: calculated from measured profile; bottom: measured by the probe vehicle.

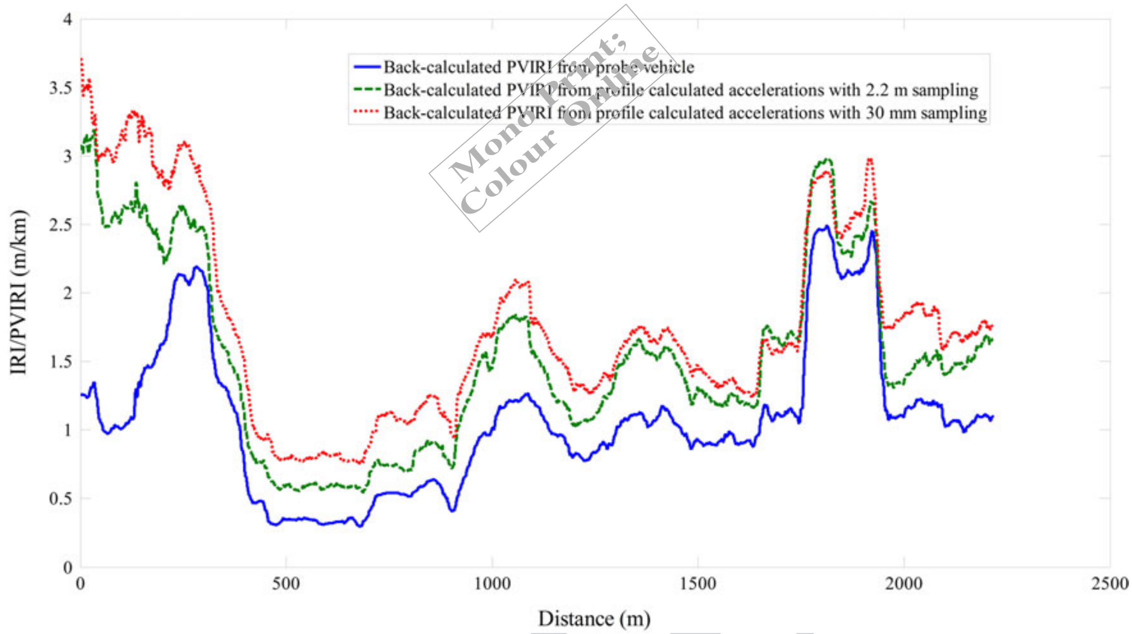

Figure 5. Calculated PVRI.

accelerations is generally lower than the PVRI calculated directly from the profile without sampling, as shown in Figure 5. This is expected as the sampled acceleration loses some of the features which results in a lower PVRI. Since the calculated PVRI at any point depends on the profile at that point as well as the profile before that point, it is not necessary that the sampled PVRI is always lower than the directly calculated PVRI. This is also evident in Figure 5.

The PVRI calculated from the probe vehicle accelerations is lower than both PVRIs calculated from the measured road profile. This was expected since the calculated accelerations from the measured profile are larger than the probe vehicle measured accelerations (shown in Figure 4). Despite that the PVRIs are shown to be similar with a correlation of 0.86 (using the PVRI of the profile sampled at 2.2 m), which is relatively good. Correlation, however, does not reveal the difference between the two PVRIs. The root mean square difference between the probe vehicle PVRI and the profile calculated PVRI sampled at 2.2 m is 0.57 m/km. A significant amount of the calculated discrepancy is caused by the difference between the PVRIs between 0 m and 250 m. This section of the pavement is a continuously reinforced concrete section which has grinding and grooving. The grinding and grooving causes single spot laser profilers (which is the type used to obtain the measurements) to measure a rough road profile that is not captured by the probe vehicle. The sensitivity analysis presented later in Figure 8 shows that this first 250-m section was the most sensitive to sampling error which is expected with grinding and grooving.

6.2 *Full car filtering*

In this section, we average the response of the front and back tyre responses. This approach should be closer to the probe vehicle measured response which accounts for the whole vehicle response. To do so, we take the original profile, shift it by a distance equal to the vehicle wheelbase length and calculate a new profile which is the average of the original profile and the shifted profile. The wheelbase length of the used probe vehicle (Ford Fusion) is 2.72 m. [AQ3] The acceleration measurements are more closely matched, as compared in Figure 6. The correlation is 0.70 which is slightly lower than the 0.73 calculated earlier. However, the average strength of the calculated acceleration from the profile is now 0.45 m/s^2 compared to 0.45 m/s^2 (that of the probe vehicle measured acceleration) with a difference of 0.8% (rounding). This is significantly lower than the 20% difference found earlier when only the left and right wheel path profiles were averaged.

Again, three PVRI sets are presented in Figure 7. One PVRI is back-calculated from the probe vehicle measured accelerations. The other two PVRI sets are calculated from the measured profile. The first profile-calculated PVRI is calculated by averaging the left and right wheel path responses in the front and the back (all tyres). The other profile PVRI accounts for only the front axle responses (average of left and right wheel paths). Clearly, the PVRI calculated from the averaged profile over all tyres more closely agree with the probe vehicle-calculated PVRI. This is because the probe vehicle is affected by the response of all four tyres. The mean

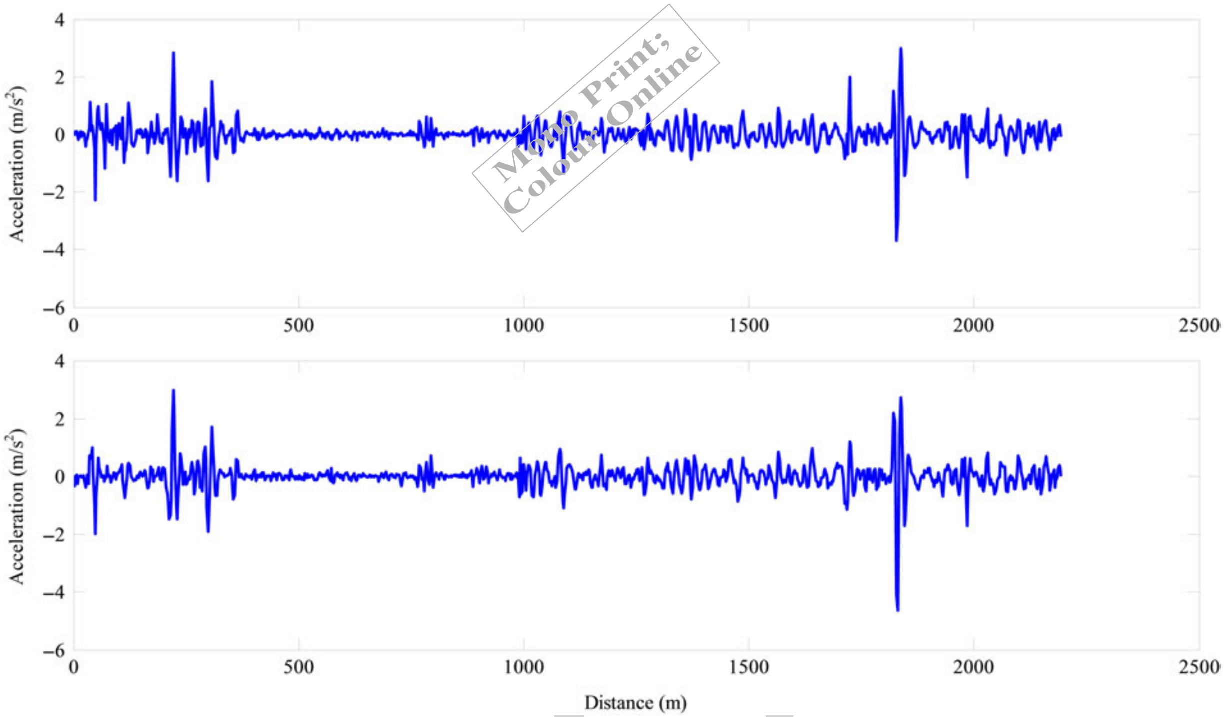

Figure 6. Vehicle vertical acceleration: (a) calculated from measured profile with front and back tyre averaging and (b) measured by the probe vehicle.

square difference between the two profiles is 0.34 m/km which is significantly smaller than the 0.57 m/km obtained when no averaging of the front and back tyres response is performed. On average, over the whole tested road, the PVRI calculated from the probe vehicle is 0.1435 m/km lower than PVRI calculated from the measured profile. The correlation between the two signals negligibly decreased to 0.84 compared to 0.86.

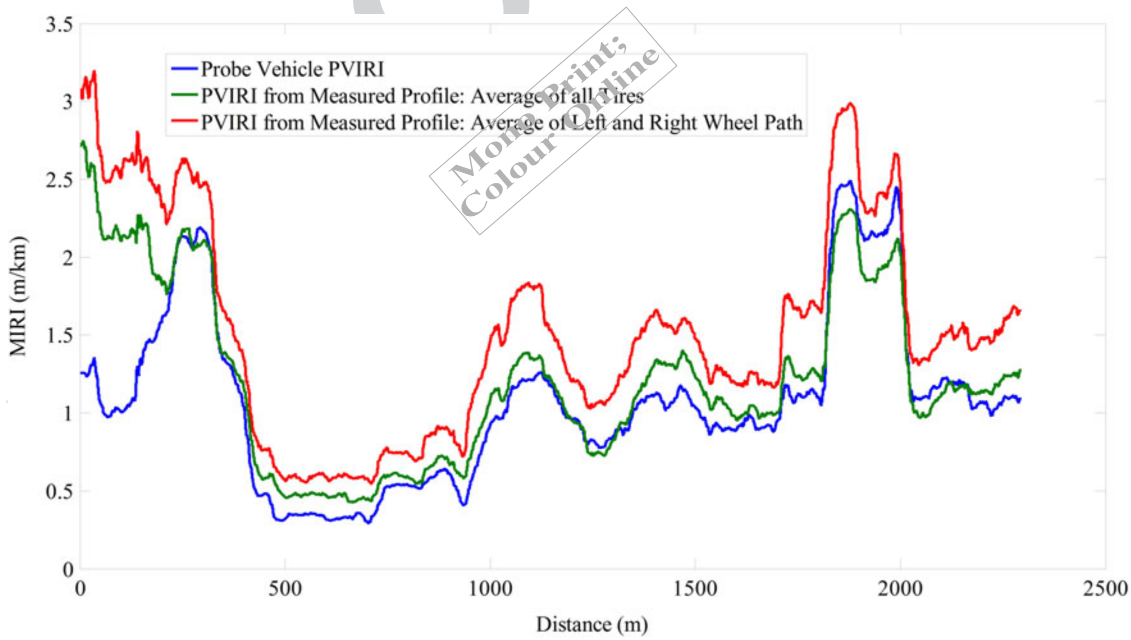

Figure 7. Calculated PVRI with front and back tyre averaging.

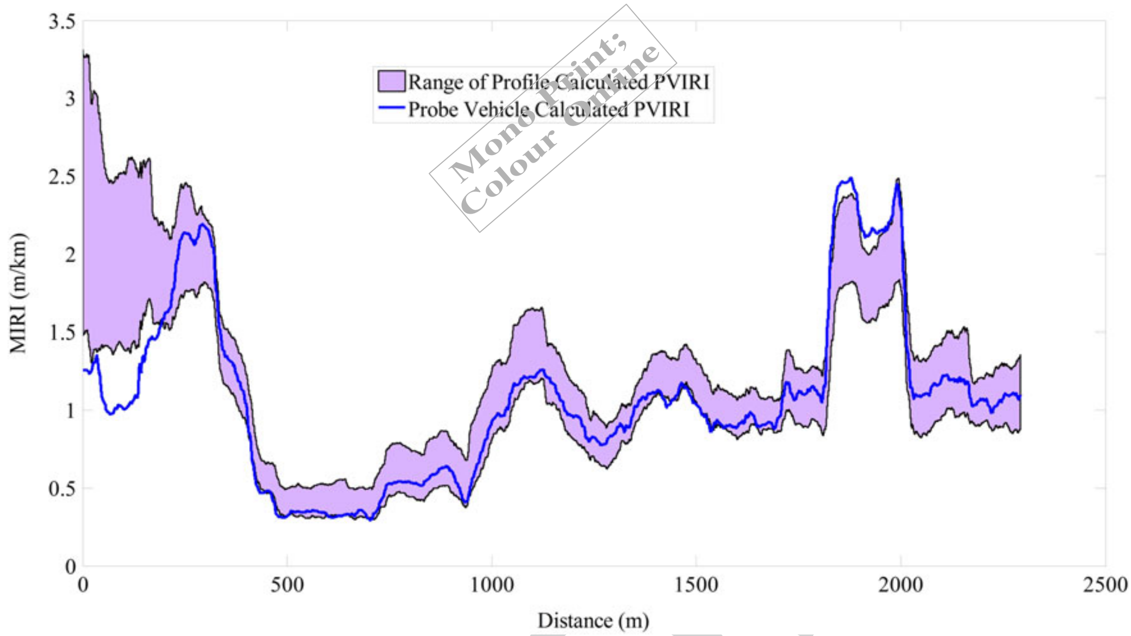

Figure 8. Effect of sampling error on calculated PVRI.

6.3. *Sensitivity to data sampling*

In this section, a sensitivity analysis of the PVRI with respect to accuracy of data sampling and with respect to the quarter car model parameters is performed. The variation of the PVRI with respect to these parameters is compared to the mean square difference of 0.17 m/km observed between the profile-calculated PVRI and the probe vehicle-calculated PVRI.

Probe vehicle measurements were obtained at a constant sampling time interval of 10 Hz. Profile measurements were obtained at a constant spatial sampling interval of 30 mm (1.2 in.). This resulted in some discrepancies between the spatial coordinate readings of the probe vehicle and the profiler. Even after shifting the probe vehicle acceleration measurements and the acceleration calculated from the profile, the peaks between the two data series did not match. A simulation (500 iterations) is performed to evaluate the effect of discrepancies between the spatial coordinate readings. Instead of sampling the profile-calculated acceleration at the spatial coordinate of the probe vehicle, we added an error term to the sampling, as shown in Equation (10):

$$x_s = x_p + \varepsilon, \tag{10}$$

where x_s is the spatial location of sampled acceleration calculated from the profile, x_p is the measured spatial location of probe vehicle acceleration measurement and ε is the discrepancy between spatial coordinate readings, uniformly distributed between -1 and 1 m.

The error is assumed to be uniform rather than normally distributed to limit the maximum deviation to <1 m. This will also insure that the location coordinate of sampled points is strictly increasing. Figure 8 shows that the sampling error can result in a considerable change in the calculated PVRI. Probe vehicle calculated PVRI is very close to the range of variation of the profile calculated PVRI. It falls within that range 75% of the time.

6.3. *Sensitivity to quarter car model parameters*

The golden car parameters are assumed for the probe vehicle (Ford Fusion). In this section, we perform a sensitivity analysis by varying the golden car parameters uniformly within a ±25% range. Figure 9 shows the variation of the probe vehicle PVRI that is due to the change of the quarter car model parameters. Also shown in Figure 9 is the variation of the profile calculated PVRI as a function of sampling, which was evaluated in Section 6.2 [AQ4] (see also Figure 6). The dark-shaded area represents the area were both ranges overlap. There is a significant amount of overlap between the two ranges (more than 95% of the road). The medium-shaded area represents the range due to sampling that does not overlap with that due to quarter car parameters' variation. The lightest-shaded area represents the range due to the variation of the quarter car parameters that does not overlap with that due to sampling. The PVRI sensitivity to the quarter car parameters is highest over rough sections, as shown in Figure 9.

To determine the individual effect of the quarter car parameters, the same simulation is performed by

GPAV 1014815—13/2/2015—PRABHAKARAN.MN—506182——Style 4

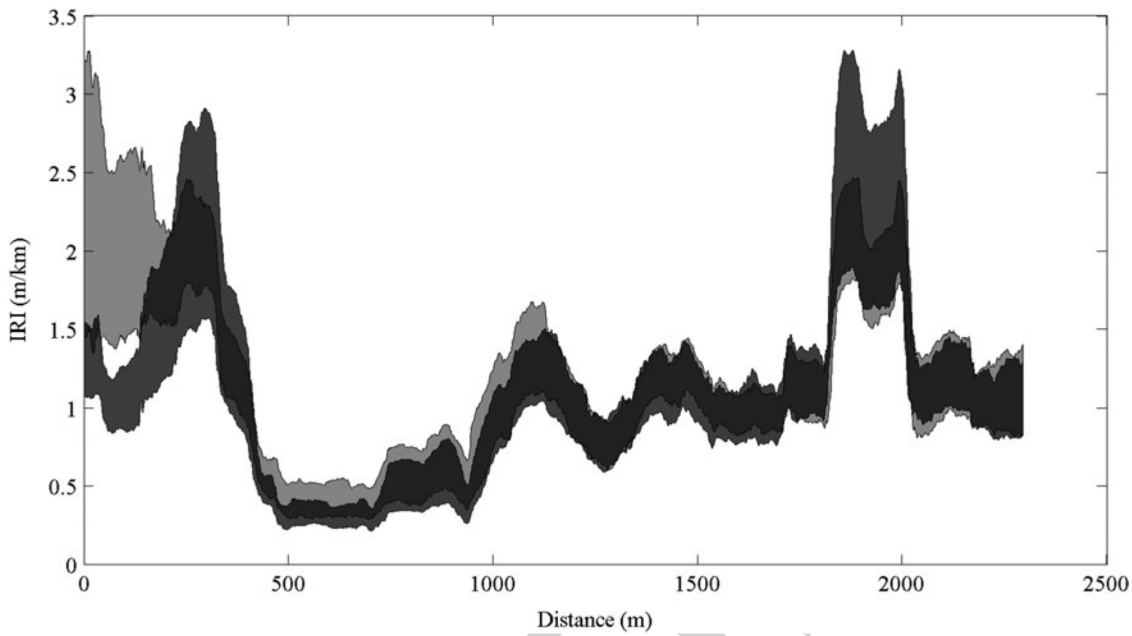

Figure 9. Effect of sampling error and quarter car parameters on calculated PVRI.

changing, within 25%, only one of the parameters at a time while holding the others at their original values. The results of this simulation are presented in Figure 10. The suspension stiffness and ratio of vehicle tyre mass to body mass had little effect on the calculated PVRI. The parameters that most affected the vehicle response are the tyre stiffness followed by the suspension damping.

The results presented here show that although there is some difference between the profile-calculated PVRI and the probe vehicle-calculated PVRI, this difference is captured by the sensitivity of the PVRI to errors in location sampling and by the variation in the quarter car parameter values.

7. Conclusions and recommendations

In this article, we compared roadway roughness measures obtained from probe vehicle and from measured profile. Two roughness measures were compared: vehicle vertical acceleration and PVRI. In general, roughness measures obtained from the profile are comparable to roughness

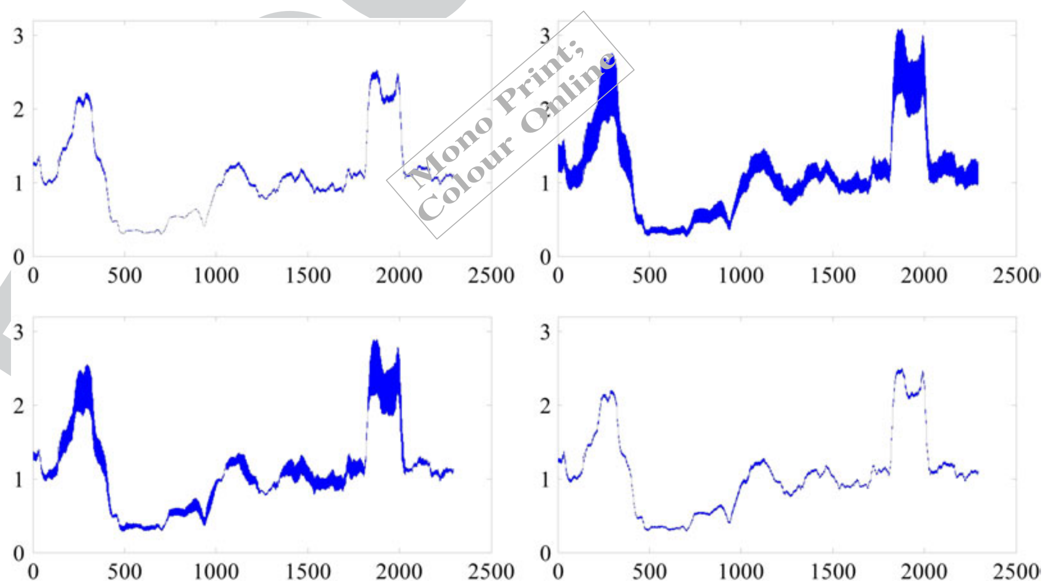

Figure 10. Effect of quarter car parameters on PVRI; top left: k_1; top right: C; bottom left: k_2; bottom right: μ.

measures obtained from the probe vehicle, when the appropriate parameters that affect roughness are taken into account. It is most important to note that probe vehicle measured roughness represents the response of the full car (all tyres) and not that of a quarter car. We also investigated the effect of the sampling frequency on the calculated PVRI. The sampling frequency of the probe vehicle was 10 Hz which corresponded to an interval of 2200 mm at 80 km/h. This interval is too large to fully capture all the features that affect the calculation of the PVRI. A sensitivity analysis with respect to the data sampling and quarter car parameters suggested that these two parameters could account for most of the discrepancies observed between the two PVRI sets.

Because the calculated PVRI depends on the sampling rate, we recommend that future probe vehicle acceleration measurements be obtained at a rate of the order of 1000 Hz. The effect of vehicle speed could also be an important parameter to evaluate especially if suspension stiffness and damping are highly nonlinear. Finally, probe vehicle measurements obtained from other vehicle types and makes should be obtained to evaluate the effect it will have on measured roadway roughness.

Funding

This research was funded by the Connected Vehicle/Infrastructure – University Transportation Center.

Notes

1. Email: skaticha@vtti.vt.edu
2. ~~Local address: P.O. Box 36, Byblos, Lebanon.~~

References

[AQ5]

Dawkins, J., *et al.*, 2011. *Investigation of pavement maintenance applications of intellidrive SM (final report): implementation and deployment factors for vehicle probe-based pavement maintenance*. Auburn University. Available from: http://cts.virginia.edu/PFS_PMSA99_Final.pdf [Accessed 15 July 2013]. [AQ6]

El Khoury, J., *et al.*, 2014. A microscale evaluation of pavement roughness effects for asset management. *International Journal of Pavement Engineering*, 15 (4), 323–333. doi:10.1080/10298436.2013.792930.

Eriksson, J., *et al.*, 2008. The pothole patrol: using a mobile sensor network for road surface monitoring. *In*: *The Sixth International Conference on Mobile Systems, Applications, and Services*. Breckenridge, CO: MobiSys. [AQ7]

Flintsch, G.W. and McGhee, K., 2009. *NCHRP synthesis 401 – quality management of pavement condition data collection*. Washington, DC: Transportation Research Board of National Academies, NAS-NRC.

Flintsch, G.W., *et al.*, 2012. Probe vehicles used to measure road ride quality. *Transportation Research Record: Journal of the Transportation Research Board*, 2304 (1), 158–165. doi:10.3141/2304-18.

Loizos, A. and Plati, C., 2008. An alternative approach to pavement roughness evaluation. *International Journal of Pavement Engineering*, 9 (1), 69–78, doi:10.1080/10298430600949894.

Ndoye, M., *et al.*, 2009. A recursive multi-scale correlation-averaging algorithm for synchronization and fusion of independent pavement roughness measurements. *In*: *12th International IEEE Conference on Intelligent Transportation Systems*. St Louis, MO: IEEE. [AQ8]

Sayers, M.W. and Karamihas, S., 1996. *Interpretation of road roughness profile data – final report UMTRI 96-19*. Ann Harbor, MI: University of Michigan.

Sayers, M.W. and Karamihas, S., 1998. *The little book of profiling*. Ann Harbor, MI: University of Michigan. Available from: http://www.umtri.umich.edu/content/LittleBook98R.pdf [Accessed 10 July 2013].